

One effective method to slow down metal corrosion rate is the impressed current cathodic protection (ICCP) system. The ICCP system is suitable for coastal applications such as piping systems and offshore structures. In this application, metal surfaces tend to be exposed to seawater. Specific concentrations of seawater can accelerate the occurrence of corrosion of metals, even though they are stainless steel types. This study applied the automatic ICCP system to stainless steel 303. Stainless steel 303 will be immersed in simulated seawater at several concentrations of NaCl (27 ppt, 31 ppt, and 35 ppt). The specimens were immersed in NaCl solution for three weeks or about 504 hours at a constant temperature of 38 °C. After the sample has been soaked, quantitative and qualitative measurements were carried out. Quantitative measures include average weight loss, corrosion rate, and potential value. At the same time, the qualitative measurements include macroscopic, Scanning Electron Microscopy (SEM), and Energy Dispersive X-Ray Spectroscopy (EDS). Based on quantitative measures, it was found that the difference in average weight loss and corrosion rate for each NaCl concentration was not very significant. The difference of each parameter is less than 0.1 % and 0.22 %, respectively. The potential value quickly reaches a steady state at NaCl concentrations of 27 ppt and 31 ppt in less than 10 seconds. The results of the SEM test showed a change in the metal structure. The oxygen (O) content in the metal after the EDS test showed a decrease in this element up to 35 % at a NaCl concentration of 35 ppt. The decrease in oxygen (O) can slow down the corrosion rate in metals when exposed to seawater

**Keywords:** corrosion rate, impressed current cathodic protection (ICCP), simulated seawater, stainless steel 303

# SUPPRESSION OF CORROSION ON STAINLESS STEEL 303 WITH AUTOMATIC IMPRESSED CURRENT CATHODIC PROTECTION (A-ICCP) METHOD IN SIMULATED SEAWATER

**Hamsir**

Doctoral Student\*

**Onny Sutresman**

Doctorate, Professor\*

**Hairul Arsyad**

Corresponding Author

Doctorate, Assistant Professor\*

E-mail: arsyad.hairul@yahoo.com

**Muhammad Syahid**

Doctorate, Assistant Professor\*

**Agus Widianto**

Doctorate, Head of Autobody Workshop and Painting Laboratory

Department of Automotive Engineering Education

Universitas Negeri Yogyakarta

Jl. Colombo No. 1, Karang Gayam, Caturtunggal, Kec. Depok, Kabupaten Sleman, Daerah Istimewa Yogyakarta, Indonesia, 55281

\*Departement of Mechanical Engineering

Hasanuddin University

Jl. Poros Malino KM., 6, Bontomarannu Gowa,

Sulawesi Selatan, Indonesia, 92171

Received date 07.09.2022

Accepted date 11.11.2022

Published date 30.12.2022

**How to Cite:** Hamsir, Sutresman, O., Arsyad, H., Syahid, M., Widianto, A. (2022). Suppression of corrosion on stainless steel 303 with automatic impressed current cathodic protection (A-ICCP) method in simulated seawater. *Eastern-European Journal of Enterprise Technologies*, 6 (12 (120)), 13–21. doi: <https://doi.org/10.15587/1729-4061.2022.267264>

## 1. Introduction

Corrosion is one of the problems that cause losses in the industry. Corrosion damage, such as material failure, device failure, and operating system failure, has a significant economic impact. In Indonesia, losses due to corrosion are estimated at trillions of rupiah. This calculation includes maintenance costs, material replacement, working hours, lost profits due to production stoppages, customer disappointment, administrative fees, physical losses, and disposal. Therefore, corrosion must be controlled, which is very important for the economy and security [1].

Corrosion cannot be eliminated but can be prevented by protecting the material from the environment. One of them is the cathodic protection of the sacrificial anode system. The cathodic protection of the sacrificial anode system has

been widely used. The design used combines experience and experimental data [2]. However, failure of cathodic protection will impact economic losses and the safety of human life and the environment.

Metal is one type of material that is widely used in industry. However, metal can be damaged by corrosion. Corrosion is an electrochemical reaction between a metal and its environment that causes rust and metal degradation [3]. The most widely used metal material in the industry is steel, and each steel has properties depending on the alloying elements it contains. Nickel (Ni), chromium (Cr), and manganese (Mn) are alloying elements that increase the corrosion resistance of steel. Based on the crystal structure, stainless steels are classified into five groups: austenitic stainless steels, ferritic stainless steels, martensitic stainless steels, duplex stainless steels, precipitation hardening

stainless steels, welded and non-ferromagnetic. Austenitic stainless steels containing the Cr and Ni elements are given serial numbers 300 and 200 for Cr, Ni, and Mn [4]. One type of austenitic stainless steel widely used in industrial and non-industrial sectors is the SS 304 series. This type of steel can be used in various industries such as chemical, food, and pharmaceutical [5].

Although stainless steel is resistant to corrosion, it can still be attacked by corrosion such as uniform corrosion, pitting corrosion or stress corrosion cracking. An extract from white tea was developed for the corrosion protection of mild steel materials [6]. The results show that white tea extract can reduce the corrosion rate by up to 85 %. Pitting corrosion is common in austenitic steel. The effect of niobium and solution treatment was investigated [7]. Niobium has better stability in reducing pitting corrosion. Thus, research is needed on the corrosion resistance of stainless steel itself. A corrosion resistance test was conducted on stainless steel 304 by reacting it in an acid solution [8]. SS 304 steel and sulfuric acid reaction causes significant pitting corrosion on metal surfaces. On the other hand, adding NaCl can reduce pitting corrosion, but the corrosion rate increases [9]. In addition to the concentration of the corrosive medium, the corrosion rate is also influenced by temperature and immersion time [10].

Several studies are still conducting experiments to prolong the life of metal from corrosion. The focus of metal used is stainless steel because it has good corrosion resistance. However, some conditions cause stainless steel to corrode. So, research to identify the right method to slow down the corrosion rate on stainless steel is still relevant.

---

## 2. Literature review and problem statement

---

Two metals that are connected electrically and then immersed in an electrolyte (seawater) are the principle of cathodic protection. The difference in electric potential causes electrons to flow from the active metal to the other metal. There are two metals, the anode and the cathode, where the cathode is connected to the metal/specimen while the anode is immersed in the electrolyte. The anode is a more active metal, while the cathode is a less active metal, so when an electric current flows, it will dissolve into ions towards the cathode [11]. This provides protection against corrosion of the metal immersed in the electrolyte.

Corrosion is a decrease in metal quality due to an electrochemical reaction with its environment. Corrosion is a process experienced by a metal that reacts electrochemically with its environment. Currently, metals are widely used by various industries. One of the widely used metals is austenitic stainless steel 303. Austenitic stainless steel generally consists of 2 types: type 200 and type 300. Stainless steel 201 and stainless steel 304 are the types that are widely used because they have good corrosion resistance properties. Stainless steels 201 and 304 can be considered substitutes for each other in some applications. Therefore, it is necessary to conduct testing to determine which metals are easy and difficult to degrade due to electrochemical reactions between metals and their environment. One way to reduce the potential for metal degradation due to the corrosion process is the addition of inhibitors in the system. The addition of inhibitors in the system is widely chosen because this method is flexible, which can provide

protection from a less aggressive environment to a highly corrosive environment. In addition, this method is easy to use and effective because it costs little but provides broad protection. Many substances can be used as inhibitors to reduce the corrosion rate, one of which is a substance that can bind oxygen in the environment to reduce the corrosion process.

The corrosion of metals has been continuously explored in recent times. The study focuses on corrosion in marine, coastal, and pipeline structural fields. The corrosion flow rate in S355ML steel is used for seafront structures where an increase in the flow rate of the medium can accelerate the corrosion rate of this material [12]. Low-carbon steel with laminar and turbulent flow conditions was investigated for its corrosion effect [13], turbulent flow will increase the effect of surface roughness of the specimen and accelerate the corrosion behavior of the steel. The corrosion flow rate determines the corrosive level of the specimen [14, 15]. The flow rate was further investigated in pipelines with low-carbon steel material [16]. The results of this study indicate an increase in the corrosion rate as the flow rate increases over a certain time.

Cathodic protection is commonly used to protect structures from corrosion [17, 18]. One of the derivatives of the cathodic protection method is impressed current cathodic protection (ICCP) [19]. The advantage of ICCP is that it is more suitable for large structures and can extend the structure's life from corrosion [20]. In addition, ICCP is an effective method of corrosion protection of electrolytes [21, 22]. The numerical simulation of the ICCP method was carried out [21] by optimizing the corrosion rate parameter. Using the ICCP system, the life of the material can be extended even if it is in an electrolyte [23]. Several studies show that ICCP is still widely used for corrosion protection. However, research related to variations in seawater salinity has not been widely carried out with the ICCP system on stainless steel 303.

Several studies on suppression of the corrosion rate are applied at room temperature. Meanwhile, in offshore applications, the temperature on the sea surface, especially in southern Indonesia, the island of Java, can reach 38 °C in summer. Therefore, applying offshore piping systems using stainless steel or steel alloy materials can cause corrosion due to exposure to seawater at a specific temperature. So, a method is needed to suppress the corrosion rate that occurs in the material. All this allows us to assert that it is expedient to conduct a study on suppression of the corrosion rate of stainless steel 303 (SS 303) using the automatic impressed current cathodic protection (A-ICCP) system.

---

## 3. The aim and objectives of the study

---

The study aims to suppress the corrosion on stainless steel 303 (SS303) with the automatic impressed current cathodic protection (A-ICCP) method.

To achieve the aim, the following objectives are accomplished:

- to investigate variations in simulated seawater salinity on macroscopic morphology on stainless steel 303 (SS303) with the automatic ICCP system;
- to investigate variations in simulated seawater salinity on weight loss and corrosion rate on stainless steel 303 (SS303) with the automatic ICCP system;

- to investigate variations in simulated seawater salinity to the potential value of stainless steel 303 with the automatic ICCP system;
- to investigate variations in simulated seawater salinity on micrographs with SEM and changes in the compound elements in stainless steel 303 (SS303) with the automatic ICCP system.

**4. Materials and methods of experiment**

**4.1. Specimen preparation**

In this study, a stainless steel material with a thickness of 5 mm was used. The dimensions of the test specimen are shown in Fig. 1. The stainless steel that has been cut is then sanded using abrasive paper (with a grit of 360, 600, 800, and 1,000) and then cleaned with alcohol and distilled water to remove dirt or rust attached to the stainless steel. Testing of the chemical composition of stainless steel materials using an optical emission spectrometer (OES) is shown in Table 1.

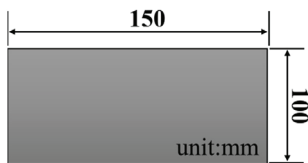


Fig. 1. Dimensions of the stainless steel specimen

Based on the results of the chemical composition test, the type of metal used is a stainless steel alloy 303 with a grade type 303 (SS 303).

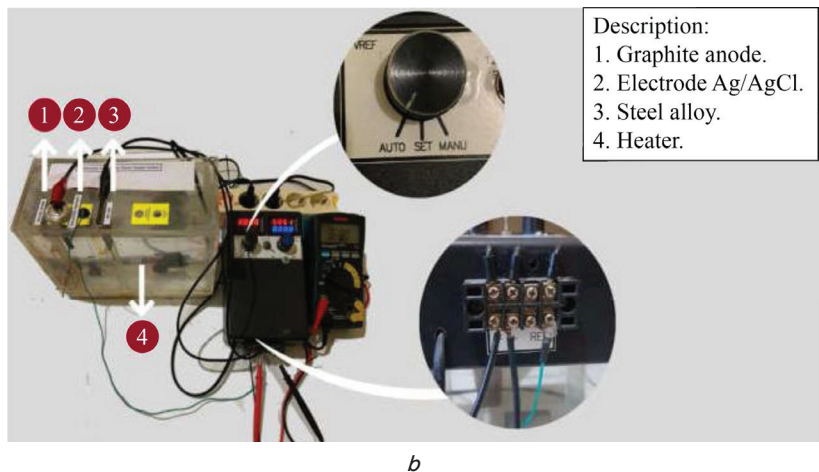
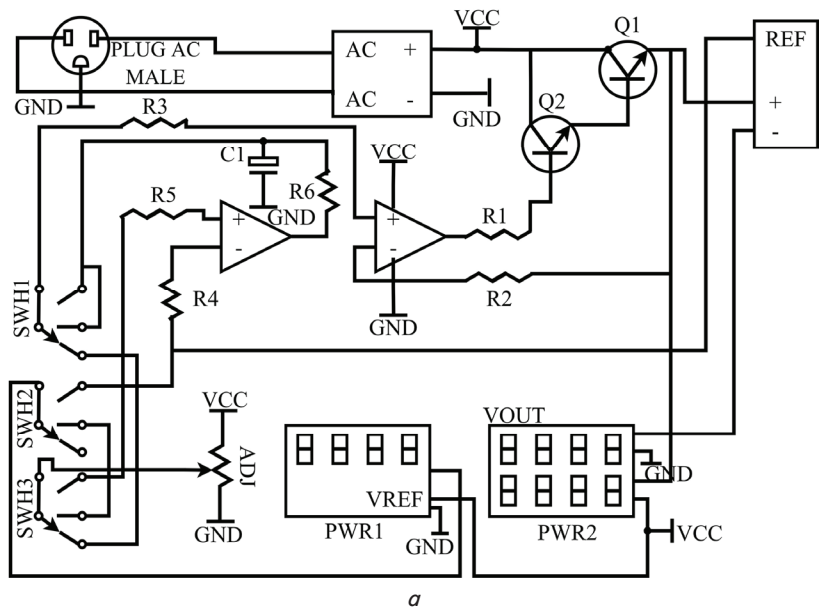


Fig. 2. Schematic of impressed current cathodic protection (ICCP): a – Electrical; b – Corrosion test system

Table 1

Chemical composition (wt %) of stainless steel 303

Stainless steel 303	C	Si	Mn	P	S	Cr	Mo
	0.0925	0.42	1.93	<0.0015	<0.001	>6.0	0.0334
	Ni	Al	Cu	Nb	Ti	V	Fe
>6.0	0.42	0.0192	0.0027	<0.0002	0.11	73.2	

**4.2. Impressed Current Cathodic Protection (ICCP) system preparation**

There are three types of simulated seawater salinity variations (concentration of NaCl), namely 27 ppt, 31 ppt, and 35 ppt. Ocean water media are made with several different levels of salinity for inclusion in stainless steel 303. In addition, an automatic forced current cathodic protection system is made to inhibit the corrosion rate.

The temperature was set constant at 38 °C. Fig. 2, a shows the electronic schematic of impressed current cathodic protection (ICCP). This ICCP system will later be applied to investigate corrosion protection efficiency on stainless steel 303 with several variations of artificial seawater salinity.

**4.3. Specimen test method**

The ICCP system as a corrosion test system used in this study is shown in Fig. 2, b. This system consists of several components: graphite anode, Ag/AgCl electrode, stainless steel 303, and heater.

Fig. 3 shows the flow of corrosion testing with the ICCP system. The first stage starts with specimen preparation, as described at the beginning of the paragraph. The next step is to test the specimen with the ICCP system corrosion test. First, the immersion of the specimens was carried out for three weeks, or about 504 hours, at a constant temperature. After that, several tests were carried out to test the results of the corrosion test specimens. Corrosion specimen testing includes quantitative and qualitative measurements.

Quantitative measurements include weight loss, corrosion rate, and potential measurement. Before the specimen is immersed into the corrosion test system, the specimen is weighed first to determine the initial mass. After that, the specimen is immersed for the specified time. The specimen is weighed again to determine the final mass when the corrosion test is finished. The weight loss can be calculated by the following formula:

$$\text{Weight loss}(W) = \frac{W_f - W_o}{W_f} \times 100\%, \tag{1}$$

where  $W_f$  and  $W_o$  are the final and initial masses in grams, respectively. Corrosion rates can be assumed over the entire specimen surface. Calculation of the corrosion rate of the specimen should be carried out as follows:

$$\text{Corrosion Rates}(CR_s) = \frac{W}{D \times A \times T} \times k, \tag{2}$$

where  $W$ ,  $D$ ,  $A$ ,  $T$ , and  $k$  are weight loss in %, specimen density in  $\text{g/cm}^3$ , specimen area in  $\text{cm}^2$ , corrosion testing time in hours, and a constant. Potential measurements were carried out on the specimen after being connected to the graphite anode and Ag/AgCl electrode. A digital voltmeter is used for this potential measurement.

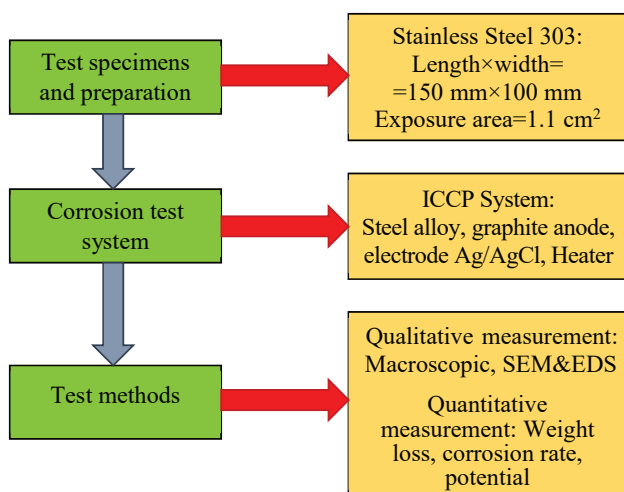


Fig. 3. Corrosion testing flowchart

Qualitative measurements include macroscopic, Scanning Electron Microscopy (SEM), and Energy Dispersive X-Ray Spectroscopy (EDS). Macroscopic observations were made before the specimen was tested for corrosion and after being tested for corrosion with several variations of artificial seawater salinity. A low-magnification digital microscope is used for macroscopic observations. The next step is SEM testing on the surface of the corroded specimen. Then changes in atomic compounds on the surface of the specimen are measured with the EDS test. After the specimens had been soaked for 504 hours, these tests were carried out.

## 5. Results of the experiment on the effect of simulated seawater on the corrosion of stainless steel 303

### 5.1. Macroscopic morphology on stainless steel 303 (SS303) with the automatic ICCP system

After being tested for corrosion for 504 hours, stainless steel 303 specimens were then visually observed for corrosion. Fig. 4 shows a macroscopic view of the specimen before and after being tested for corrosion by the ICCP system. Fig. 4, *a* is the initial condition of the specimen where there is no corrosion. At 27 ppt salinity, the specimen started to corrode at the top, as shown in Fig. 4, *b*. Furthermore, the salinity was increased to 31 ppt, where the surface of the specimen experienced severe corrosion (Fig. 4, *c*). While

Fig. 4, *d* has a salinity of 35 ppt, it can be seen that a lot of corrosion occurs on the surface of the specimen.

Research on the flow rate of electrolytes has been carried out in [24]. The research used three flow rates, namely 0.7 mL/min, 7 mL/min and 14 mL/min. The increase in the corrosion rate is very significant from the first to the third variation. The results of macroscopic observations of several variations of the electrolyte flow rate are shown in Fig. 5. With a flow rate of 0.7 mL/min in Fig. 5, *a*, the specimen begins to corrode at the edges. When the flow rate is increased 10 times, the corrosion potential will increase as expressed in Fig. 5, *b*. Subsequently, the flow rate was increased by 2 times and the entire surface of the specimen was corroded as shown in Fig. 5, *c*.

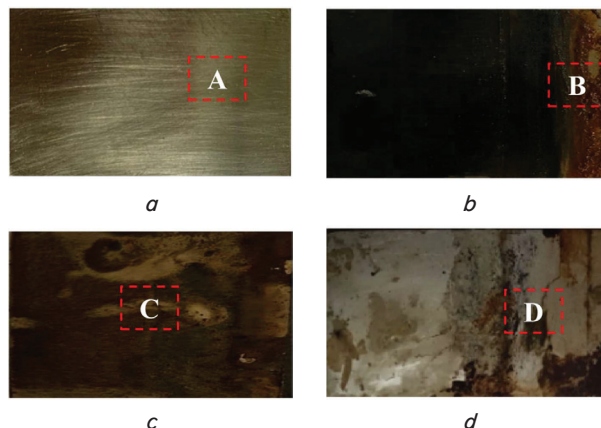


Fig. 4. Macroscopic morphology of stainless steel 303: *a* – before the test; *b* – 27 ppt; *c* – 31 ppt; *d* – 35 ppt

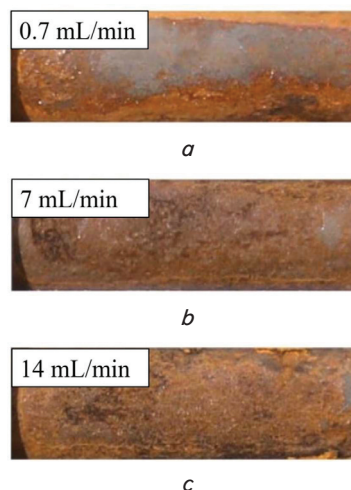


Fig. 5. Morphology macrograph at different electrolyte flow rates [24]: *a* – 0.7 mL/min; *b* – 7 mL/min; *c* – 14 mL/min

This study shows that the NaCl concentration parameter influences the corrosion rate. In another study, the electrolyte flow rate also affects the corrosion rate. Stainless steel 303 with corrosion resistance can also have its surface corroded if exposed to liquid electrolytes at a specific concentration or flow rate. So the ICCP system can slow down the corrosion rate in stainless steel 303.

### 5.2. Weight loss and corrosion rate on stainless steel 303 (SS303) with the automatic ICCP system

Weight loss is a quantitative measure of the average corrosion rate as the difference between the specimen's initial

mass and the specimen's final mass. Fig. 6, *a* shows the average weight loss in several variations of artificial seawater salinity. For example, samples with 27 ppt have a weight loss of 0.00915 g, while the weight loss at 31 ppt and 35 ppt is 0.00917 g and 0.00917 g, respectively. The average weight loss of the three samples did not differ much less than 0.1 %. Based on the average weight loss results, the salinity parameter of 31 ppt is the largest in weight loss.

Corrosion rates for the salinity of 27 ppt, 31 ppt, and 35 ppt are presented in Fig. 6, *b*. The corrosion rate of the three samples was not much less than 0.001 mmpy. Therefore, salinity 27 ppt corrosion rate that occurs is 0.24002 mmpy. Then for the salinity of 31 ppt and 35 ppt, the corrosion rates were 0.24107 mmpy and 0.24055 mmpy, respectively. So, the corrosion rate with a salinity of 31 ppt is the largest among other salinity parameters.

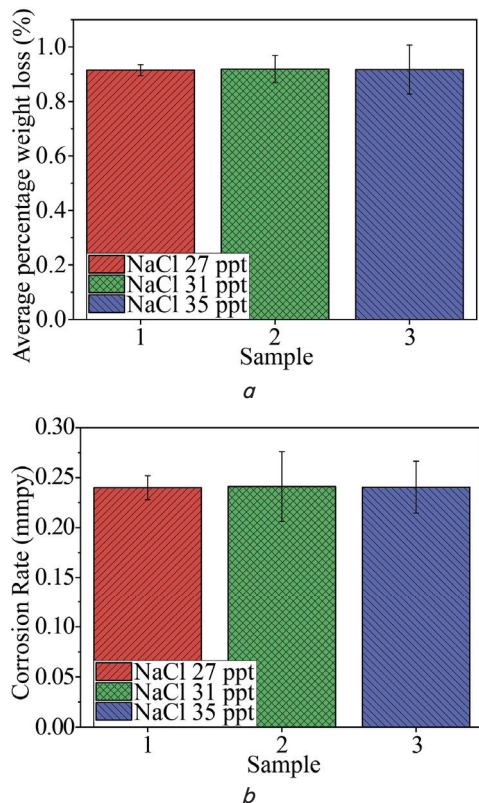


Fig. 6. Quantitative measurement: *a* – average percentage weight loss; *b* – corrosion rate

### 5.3. Potential measurement on stainless steel 303 (SS303) with the automatic ICCP system

The potential value for corrosion and steel protection in the seawater environment using the Ag/AgCl reference electrode is in the minimum range of  $-0.800$  V to  $-1.100$  V. If it is more negative than  $-1.100$  V, it will generate hydroxy ions, which results in a very wet environment and high pH. This can lead to the start of cathodic release in the metal layer. Fig. 7 shows the results of measuring potential values during the ICCP process.

The measurement of the potential value on the sample was carried out for 60 seconds at a salinity of 27 ppt, 31 ppt, and 35 ppt. Salinity at 31 ppt gives the smallest potential value, while salinity at 35 ppt gives the greatest potential value. Therefore, the potential value will be the steady state at 10 seconds at a salinity of 27 ppt and 31 ppt. However, for 35 ppt salinity, the potential value goes up and down every 10 seconds.

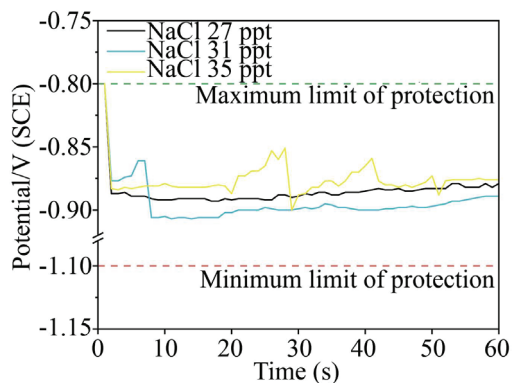


Fig. 7. The curve of potential stainless steel 303 in some seawater salinity

### 5.4. Scanning Electron Microscopy and Energy Dispersive X-Ray Spectroscopy on stainless steel 303 (SS303) with the automatic ICCP system

Scanning Electron Microscopy (SEM) observations were carried out to see the morphology of the surface micrograph of the specimen. Fig. 8, *a* shows the results of SEM observations before the specimen was tested for corrosion according to the red box in Fig. 4, *a*. SEM observations show no visible corrosion because the specimen has not been immersed in seawater.

The red box in Fig. 8, *a* is then used for the EDS test area, the results of the EDS test are presented in Fig. 8, *b*. The display of the EDS test results of stainless steel 303 samples before immersion shows some chemical elements such as iron (Fe), oxygen (O), chromium (Cr), nickel (Ni), magnesium (Mg) and silicon (Si). The element that is dominant in stainless steel 303 is iron (68.44 %). The iron element is susceptible to corrosion, so automatic ICCP is hoped to suppress the corrosion rate.

SEM observed a salinity of 27 ppt on the specimen surface in the red box area in Fig. 4, *b*. The results of the micrograph of the specimen surface are shown in Fig. 9, *a*. There is visible corrosion in some areas. EDS then tests the red box area in Fig. 9, *a* to determine changes in the compound after corrosion occurs on the metal surface. Fig. 9, *b* shows the results of the EDS test at a salinity of 27 ppt.

The results of the EDS test on stainless steel 303 samples with auto-cathodic protection treatment showed several chemical elements, including oxygen (O), sodium (Na), magnesium (Mg), silicon (Si), sulfur (S), chlorine (Cl), chromium (Cr), manganese (Mn), iron (Fe) and nickel (Ni). One of the corrosion products whose value is reduced is oxygen – by 23.94 %, so reducing the amount of oxygen in the material can directly reduce the corrosion rate. The iron content is also still high, around 51.28 %, so the corrosion rate can be well controlled from this EDS data.

Observation of the corroded surface in the red box area of Fig. 4, *c* continued with SEM testing. With a salinity of 31 ppt, it can be seen that the entire surface is corroded. Fig. 10, *a* shows the results of surface observations with SEM at a salinity of 31 ppt. Furthermore, the red box area in Fig. 10, *a* was observed with EDS to determine changes in the compound after corrosion occurred. The results of the EDS test at a salinity of 31 ppt are presented in Fig. 10, *b*.

The EDS results provide information related to the elements contained in the automatic ICCP stainless steel 303 material in synthetic seawater with NaCl 31 ppt and a temperature of  $38$  °C, namely elements of carbon (C), oxygen (O), sodium (Na), silicon (Si), chlorine (Cl), chro-

mium (Cr), iron (Fe) and nickel (Ni). In this condition, the oxygen element is still in approximately the same amount as the NaCl condition of 27 ppt of 24.37 %. However, the iron content was much reduced from the previous condition of 10.30 %, much smaller than the experiment at 27 ppt.

Fig. 4, *d* has a red box, which is the SEM testing area. Based on micrograph observations, it can be seen that some corrosion is shown in Fig. 11, *a*. Furthermore, the EDS test is carried out in area IV in the red box in Fig. 11, *a*. Finally, the results of the EDS test for 35 ppt salinity are shown in Fig. 11, *b*.

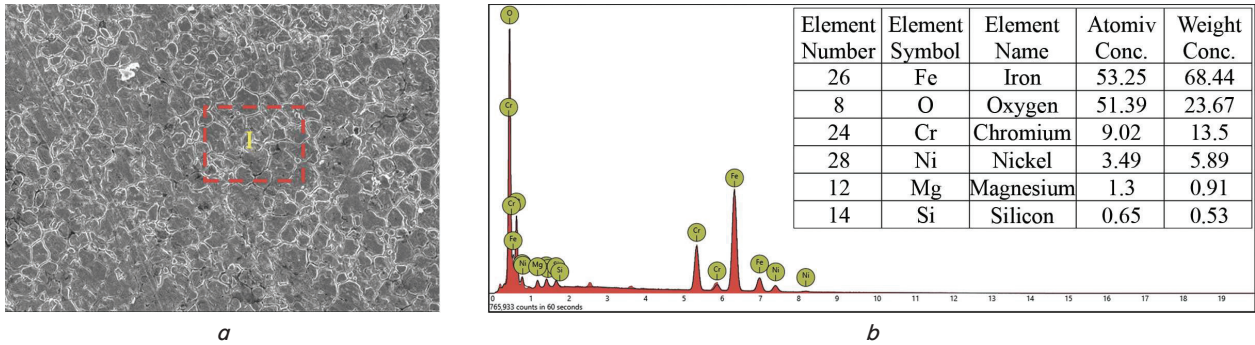


Fig. 8. Qualitative measurement: *a* – micrograph with Scanning Electron Microscope; *b* – Energy Dispersive X-Ray Spectroscopy before corrosion test

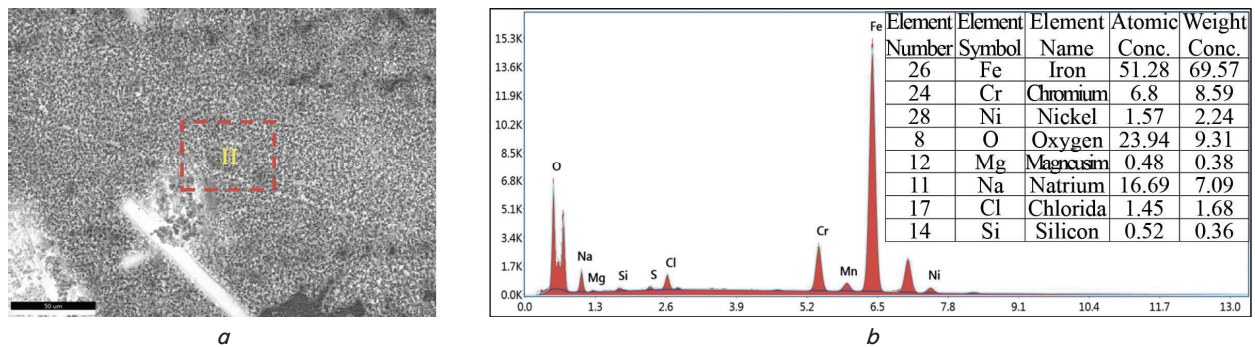


Fig. 9. Qualitative measurement: *a* – micrograph with Scanning Electron Microscope; *b* – Energy Dispersive X-Ray Spectroscopy for 27 ppt salinity

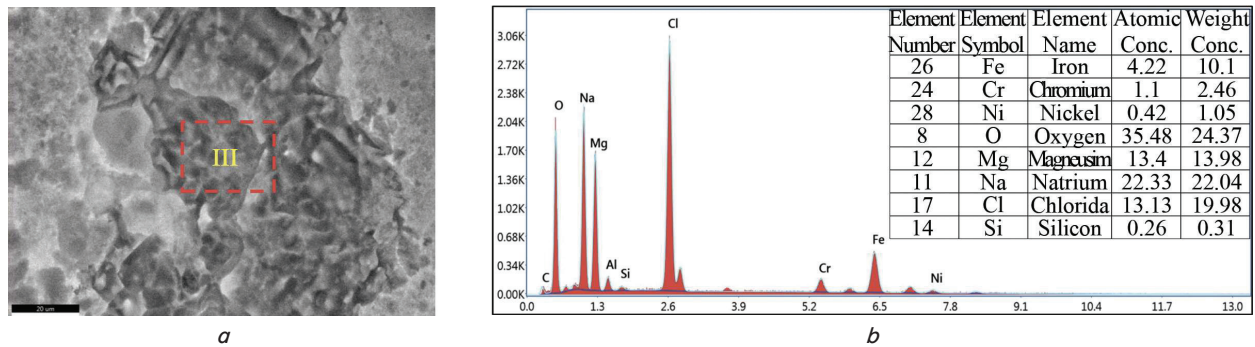


Fig. 10. Qualitative measurement: *a* – micrograph with Scanning Electron Microscope; *b* – Energy Dispersive X-Ray Spectroscopy for 31 ppt salinity

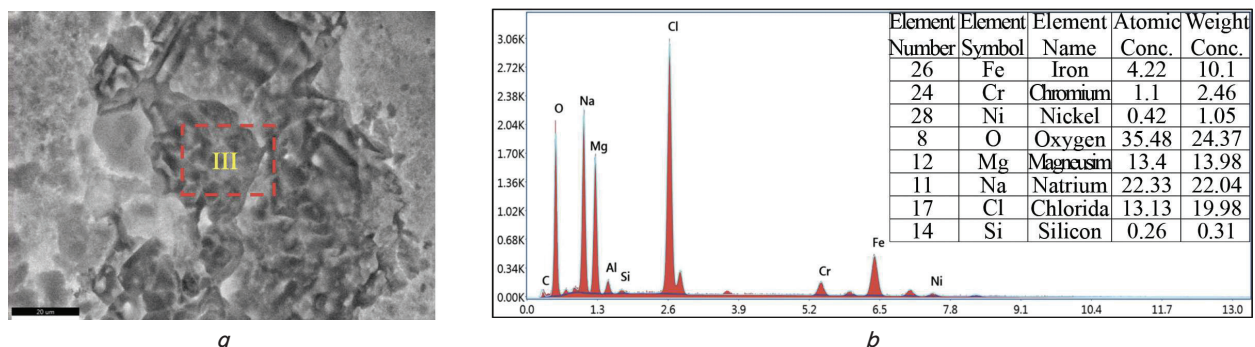


Fig. 10. Qualitative measurement: *a* – micrograph with Scanning Electron Microscope; *b* – Energy Dispersive X-Ray Spectroscopy for 31 ppt salinity

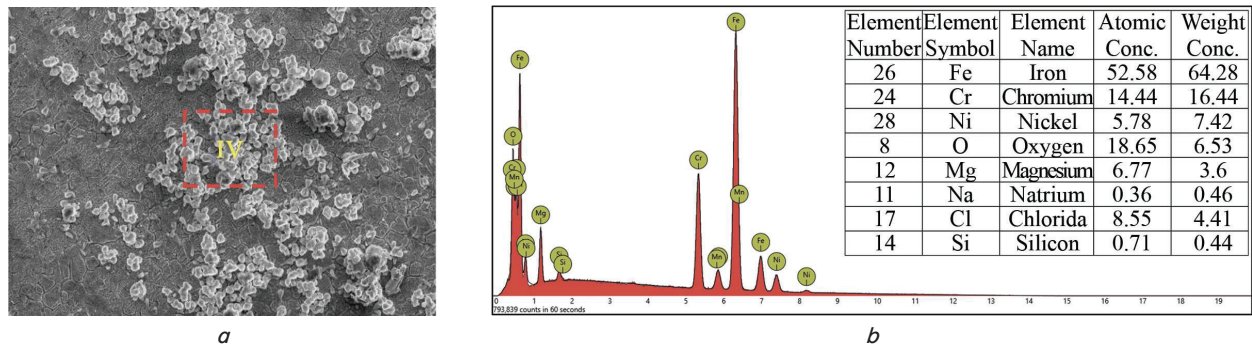


Fig. 11. Qualitative measurement: *a* – micrograph with Scanning Electron Microscope; *b* – Energy Dispersive X-Ray Spectroscopy for 35 ppt salinity

EDS results for stainless steel 303 samples immersed in synthetic seawater with 35 ppt salinity and in automatic ICCP are presented. The chemical elements detected were iron (Fe), chromium (Cr), nickel (Ni), oxygen (O), magnesium (Mg), manganese (Mn), and silicon (Si). One of the reduced corrosion products is oxygen – by 18.65 %, smaller than the previous conditions, both at 27 ppt and 31 ppt. So, the corrosion rate on the material can be more maximally controlled. The reduced oxygen element decreases the hydrogen embrittlement process.

## 6. Discussion of the results of the effect of simulated seawater on corrosion of stainless steel 303

This research is based on several previous studies [11, 17, 24, 25] discussing the ICCP method to suppress the corrosion rate of metals. The ICCP method is a general method that is widely applied to reduce the corrosion rate. Rainwater/seawater simulations were carried out by several researchers using flow rate as the main parameter. In addition, some use sand on the coast in an area as a medium. Finally, some tests were carried out at room temperature due to adjustment of metal placement. So, from several studies that have been carried out, further research is needed on how to suppress the corrosion rate of stainless steel 303 at several concentrations of NaCl with high temperature conditions. This section discusses the effect of NaCl concentration on macroscopic morphology, weight loss, corrosion rate, potential value, and SEM and EDS.

The macroscopic morphology of stainless steel 303 with simulated seawater salinity of 27 ppt, 31 ppt, and 35 ppt is shown in Fig. 4. The greater the salinity of seawater, the more corrosion occurs on the metal surface. For example, at the level of NaCl concentration of 27 ppt, only the upper surface rust occurred, while at the NaCl concentration of 31 ppt and 35 ppt, rust occurred on the entire metal surface. Another study showed the same thing [24], but different parameters used the flow rate of electrolyte and on high-strength steel wire materials commonly used in bridge construction. The greater the electrolyte flow rate, the faster the corrosion process will occur. This test is based on visual results after the metal has been immersed in simulated seawater for 504 hours at a constant temperature of 28 °C. Furthermore, to analyze the effect of variations of simulated seawater on corrosion, quantitative (weight loss, corrosion rate, potential value) and qualitative (SEM & EDS) analyses were carried out.

Quantitative analysis includes calculating weight loss, corrosion rate, and potential value. Average weight loss in all

variations of salinity has a difference of less than 0.1 %. The weight loss after the corrosion test for all specimens was less than 0.001 grams. So, the salinity of simulated seawater has no significant effect on weight loss. This is because the variation in salinity used is not much different, the difference is only 0.4 ppt for each parameter. Another study showed that the immersion time of the metal and the type of electrolyte had an effect on weight loss [25]. The corrosion rate on metals in several variations of simulated seawater salinity shows a difference of less than 0.22 %. The corrosion rate of stainless steel 303 did not experience a significant difference even though they were immersed in different concentrations of NaCl. This is caused by the effect of automatic ICCP. To suppress the corrosion rate of the ICCP system, the potential value is controlled with a value range of  $-0.8$  V to  $-1.1$  V. With this potential value set, the cathodic release to the metal can be maximized. The highest concentration of NaCl is difficult to obtain a steady state potential value. At the same time, the other NaCl concentrations can reach steady state values before 10 seconds. The same phenomenon occurred in [24], where the difference in the electrolyte flow rate and the difference in potential value will affect the corrosion rate.

The results of the SEM and EDS tests showed changes in the structure and chemical elements of the metal before being immersed in NaCl solution and after being immersed in NaCl solution at various concentrations. The dominant chemical elements before the metal is immersed are iron (Fe) (53 %) and oxygen (O) (51 %). These two chemical elements influence the occurrence of corrosion. After the metal is immersed in several concentrations of NaCl, the chemical elements iron (Fe) and oxygen (O) decrease in value. The values of the chemical element iron (Fe) at concentrations of NaCl 27 ppt, 31 ppt, and 35 ppt were 51 %, 10 %, and 52 %, respectively. While the chemical element oxygen (O) with a concentration value of 27 ppt NaCl is 23 %, NaCl 31 ppt – 24 %, and NaCl 35 ppt – 18 %. So, after the metal is immersed, the value of the chemical element oxygen (O) decreases at each concentration of NaCl. By reducing the oxygen element, the corrosion rate can be controlled to the maximum. The hydrogen embrittlement process will decrease as the oxygen element decreases [26].

The results of this study indicate that the A-ICCP system can suppress the corrosion of stainless steel. In previous studies, few have discussed the effect of NaCl concentration, especially at high temperatures. Most studies were conducted at room temperature. Seawater temperature also influences the corrosion rate. The temperature of the electrolyte affects the process of corrosion. This is because as

the temperature increases, the kinetic energy of the particles also increases, so the possibility of a practical collision in a redox reaction increases. Thus, the corrosion rate of the metal increases. In addition, the salinity level of seawater (NaCl concentration) is vital in the occurrence of metal corrosion. Corrosion is oxidizing a metal with air or other electrolytes, where the air or electrolyte will undergo reduction. Compounds in nature that include electrolyte solutions are acidic rainwater or seawater containing salt. Salt is a chemical compound that either oxidizes or reduces, so the higher the level of salt, the higher the corrosion rate.

The results of this study still have some limitations. Although, for example, the potential value test is carried out only once, it is recommended to be carried out periodically at intervals of several days. This is important to determine changes in the potential value of the electrolyte solution from the ICCP system. In addition, it is necessary to conduct XRD testing to observe the composition of corrosion products with the ICCP system. Furthermore, further testing is needed to characterize the corrosion rate of metals using the electrochemical impedance spectroscopy (EIS) method. So, adding some of these tests can give a complete characterization of the corrosion rate on stainless steel 303. Some of these things can be considered for further research, both theoretically and practically.

In practical applications, the level of salinity (NaCl concentration) and sea surface temperature are important factors for metal corrosion. This is a factor that is not controlled by external factors. Further research can be carried out in advance on the coast of the level of salinity (NaCl concentration) and sea surface temperature from morning to night. So, the initial data obtained are the minimum and maximum levels of salinity and the minimum and maximum temperatures. Furthermore, these parameters were tested on a laboratory scale for several metals.

---

## 7. Conclusions

---

1. Macroscopic morphology at several NaCl concentrations showed differences. The greater the concentration of NaCl, the faster the corrosion rate will be. The metal surface is completely corroded with NaCl concentrations of 31 ppt and 35 ppt.

2. Average weight loss and corrosion rate are quantitative measures of metal after immersion in NaCl solution (27 ppt, 31 ppt, and 35 ppt). The average weight loss and corrosion rate of the three NaCl concentrations did not differ much less than 0.1 % and 0.22 %, respectively. The average weight loss starts from 0.00915 – 0.00919 grams, while the corrosion rate has a value from 0.24002 – 0.24107 mmpy.

3. The potential value is set in the range of –0.8 V to –1.1 V, where with a NaCl concentration of 35 ppt, the potential value is difficult to reach a steady state value. Meanwhile, NaCl concentrations of 27 ppt and 31 ppt can reach potential values in steady-state conditions in less than 10 seconds.

4. The SEM test shows that there is a change in metal structure due to corrosion. At the same time, the EDS test showed a decrease in the oxygen element (O) up to 35 % at a NaCl concentration of 35 ppt.

---

## Conflict of interest

---

The authors declare that they have no conflict of interest in relation to this research, whether financial, personal, authorship or otherwise, that could affect the research and its results presented in this paper.

---

## Financing

---

The study was performed without financial support.

---

## Data availability

---

Data will be made available on reasonable request.

---

## Acknowledgments

---

This research is supported by the Mechanical Engineering Laboratory, Hasanuddin University, the Jakarta National Nuclear Energy Agency laboratory, and the Mechanical Engineering Laboratory, Sepuluh November Institute Surabaya.

---

## References

1. Roberge, P. R. (2012). Handbook of corrosion engineering. McGraw-Hill Education. Available at: <https://www.accessengineeringlibrary.com/content/book/9780071750370>
2. Xiao, J., Chaudhuri, S. (2011). Predictive modeling of localized corrosion: An application to aluminum alloys. *Electrochimica Acta*, 56 (16), 5630–5641. doi: <https://doi.org/10.1016/j.electacta.2011.04.019>
3. Roberge, P. R. (2008). Corrosion engineering. McGraw-Hill. Available at: <https://www.accessengineeringlibrary.com/content/book/9780071482431>
4. Technical Handbook of Stainless Steels (2021). Atlas Steels. Available at: <https://atlassteels.com.au/wp-content/uploads/2021/08/Atlas-Steels-Technical-Handbook-of-Stainless-Steels-12-08-21.pdf>
5. Troconis, B. C., Sharp, S. R., Ozyildirim, H. C., Demarest, C. R., Wright, J., Scully, J. R. (2020). Corrosion-resistant stainless steel strands for prestressed bridge piles in marine atmospheric environments. Available at: <https://trid.trb.org/view/1693224>
6. Kaban, A. P. S., Ridhova, A., Priyotomo, G., Elya, B., Maksum, A., Sadeli, Y. et al. (2021). Development of white tea extract as green corrosion inhibitor in mild steel under 1 M hydrochloric acid solution. *Eastern-European Journal of Enterprise Technologies*, 2 (6 (110)), 6–20. doi: <https://doi.org/10.15587/1729-4061.2021.224435>
7. Bai, G., Lu, S., Li, D., Li, Y. (2016). Influences of niobium and solution treatment temperature on pitting corrosion behaviour of stabilised austenitic stainless steels. *Corrosion Science*, 108, 111–124. doi: <https://doi.org/10.1016/j.corsci.2016.03.009>



8. Loto, R. T. (2013). Pitting corrosion evaluation of austenitic stainless steel type 304 in acid chloride media. *Journal of Materials and Environmental Science*, 4 (4), 448–459. Available at: [https://www.researchgate.net/publication/272621606\\_Pitting\\_corrosion\\_evaluation\\_of\\_austenitic\\_stainless\\_steel\\_type\\_304\\_in\\_acid\\_chloride\\_media](https://www.researchgate.net/publication/272621606_Pitting_corrosion_evaluation_of_austenitic_stainless_steel_type_304_in_acid_chloride_media)
9. Loto, R. T., Loto, C. A., Popoola, A. P. I., Ranyaoa, M. (2012). Corrosion resistance of austenitic stainless steel in sulphuric acid. *International Journal of Physical Sciences*, 7 (10). doi: <https://doi.org/10.5897/ijps11.1580>
10. Iliyasu, I., Yawas, D. S., Aku, S. Y. (2012). Corrosion behavior of austenitic stainless steel in sulphuric acid at various concentrations. *Advances in Applied Science Research*, 3 (6), 3909–3915. Available at: <https://www.primescholars.com/articles/corrosion-behavior-of-austenitic-stainless-steel-in-sulphuric-acid-atvarious-concentrations.pdf>
11. Xu, L., Xin, Y., Ma, L., Zhang, H., Lin, Z., Li, X. (2021). Challenges and solutions of cathodic protection for marine ships. *Corrosion Communications*, 2, 33–40. doi: <https://doi.org/10.1016/j.corcom.2021.08.003>
12. Bahekar, P. V., Gadve, S. S. (2017). Impressed current cathodic protection of rebar in concrete using Carbon FRP laminate. *Construction and Building Materials*, 156, 242–251. doi: <https://doi.org/10.1016/j.conbuildmat.2017.08.145>
13. Evgeny, B., Hughes, T., Eskin, D. (2016). Effect of surface roughness on corrosion behaviour of low carbon steel in inhibited 4 M hydrochloric acid under laminar and turbulent flow conditions. *Corrosion Science*, 103, 196–205. doi: <https://doi.org/10.1016/j.corsci.2015.11.019>
14. Zheng, Z. B., Zheng, Y. G., Zhou, X., He, S. Y., Sun, W. H., Wang, J. Q. (2014). Determination of the critical flow velocities for erosion–corrosion of passive materials under impingement by NaCl solution containing sand. *Corrosion Science*, 88, 187–196. doi: <https://doi.org/10.1016/j.corsci.2014.07.043>
15. Liang, J., Deng, A., Xie, R., Gomez, M., Hu, J., Zhang, J. et al. (2013). Impact of flow rate on corrosion of cast iron and quality of remineralized seawater reverse osmosis (SWRO) membrane product water. *Desalination*, 322, 76–83. doi: <https://doi.org/10.1016/j.desal.2013.05.001>
16. Vasylijev, G. S. (2015). The influence of flow rate on corrosion of mild steel in hot tap water. *Corrosion Science*, 98, 33–39. doi: <https://doi.org/10.1016/j.corsci.2015.05.007>
17. Kim, Y.-S., Seok, S., Lee, J.-S., Lee, S. K., Kim, J.-G. (2018). Optimizing anode location in impressed current cathodic protection system to minimize underwater electric field using multiple linear regression analysis and artificial neural network methods. *Engineering Analysis with Boundary Elements*, 96, 84–93. doi: <https://doi.org/10.1016/j.enganabound.2018.08.012>
18. Lauria, D., Minucci, S., Mottola, F., Pagano, M., Petrarca, C. (2018). Active cathodic protection for HV power cables in undersea application. *Electric Power Systems Research*, 163, 590–598. doi: <https://doi.org/10.1016/j.epr.2017.11.016>
19. Jeong, J. A., Jin, C. K. (2014). Experimental Studies of Effectiveness of Hybrid Cathodic Protection System on the Steel in Concrete. *Science of Advanced Materials*, 6 (10), 2165–2170. doi: <https://doi.org/10.1166/sam.2014.2061>
20. Wilson, K., Jawed, M., Ngala, V. (2013). The selection and use of cathodic protection systems for the repair of reinforced concrete structures. *Construction and Building Materials*, 39, 19–25. doi: <https://doi.org/10.1016/j.conbuildmat.2012.05.037>
21. Qiao, G., Guo, B., Ou, J. (2017). Numerical Simulation to Optimize Impressed Current Cathodic Protection Systems for RC Structures. *Journal of Materials in Civil Engineering*, 29 (6). doi: [https://doi.org/10.1061/\(asce\)mt.1943-5533.0001837](https://doi.org/10.1061/(asce)mt.1943-5533.0001837)
22. Zhu, J.-H., Wei, L., Moahmoud, H., Redaelli, E., Xing, F., Bertolini, L. (2017). Investigation on CFRP as dual-functional material in chloride-contaminated solutions. *Construction and Building Materials*, 151, 127–137. doi: <https://doi.org/10.1016/j.conbuildmat.2017.05.213>
23. Christodoulou, C., Glass, G., Webb, J., Austin, S., Goodier, C. (2010). Assessing the long term benefits of Impressed Current Cathodic Protection. *Corrosion Science*, 52 (8), 2671–2679. doi: <https://doi.org/10.1016/j.corsci.2010.04.018>
24. Li, S., Zhang, L., Wang, Y., Hu, P., Jiang, N., Guo, P. et al. (2021). Effect of cathodic protection current density on corrosion rate of high-strength steel wires for stay cable in simulated dynamic marine atmospheric rainwater. *Structures*, 29, 1655–1670. doi: <https://doi.org/10.1016/j.istruc.2020.12.028>
25. Jusoh, S. M., Nik, W. M. N. W., Azman, N. A., Zulkifli, M. F. R. (2020). Corrosion Behavior of Low-Carbon Steel and Stainless Steel 304 Under Two Soil Conditions at Pantai Mengabang Telipot, Terengganu, Malaysia. *Malaysian Journal of Analytical Sciences*, 24 (6), 954–969. Available at: [https://mjas.analis.com.my/mjas/v24\\_n6/pdf/Suriani\\_24\\_6\\_14.pdf](https://mjas.analis.com.my/mjas/v24_n6/pdf/Suriani_24_6_14.pdf)
26. Thomas, S., Ott, N., Schaller, R. F., Yuwono, J. A., Volovitch, P., Sundararajan, G. et al. (2016). The effect of absorbed hydrogen on the dissolution of steel. *Heliyon*, 2 (12), e00209. doi: <https://doi.org/10.1016/j.heliyon.2016.e00209>